Supporting Information

Nothaft et al. 10.1073/pnas.0903078106

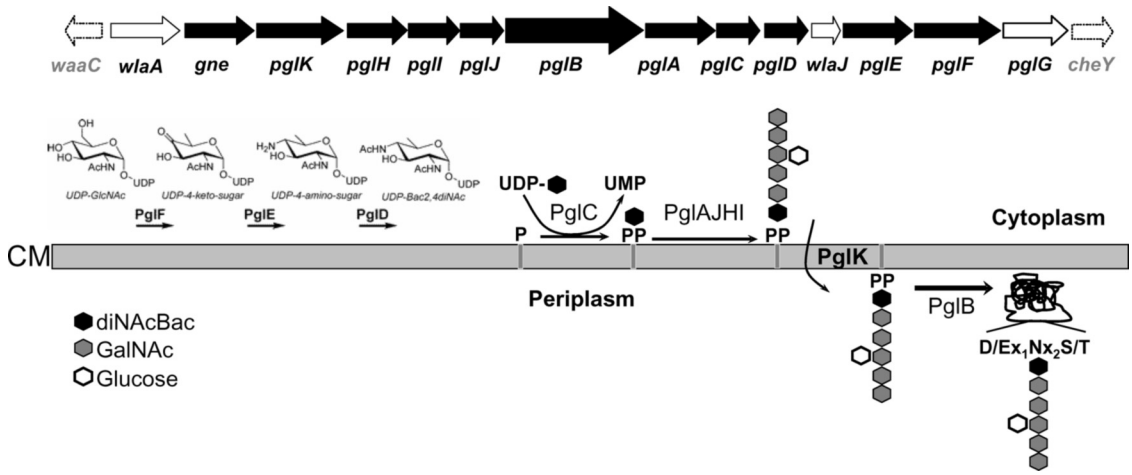

Fig. S1. *N*-linked protein glycosylation in *C. jejuni* 11168. Genes with known function in the *C. jejuni pgl* pathway are depicted in black: Gne, C4 epimerase to form GalNAc from GlcNAc; UDP activated GlcNAc is modified by PglF to form the UDP-4-keto-sugar substrate of PglE. PglE forms UDP-2-acetamido-4-amino-2,4,6-trideoxy-α-D-glycopyranose (UDP-4-amino-sugar) (1). PglD modifies the UDP-4-amino-sugar to form UDP-diNAcBac, using acetyl-CoA as the acetyl group donor (2). PglC, the first glycosyltransferase, attaches a diNAcBac-phosphate to undecaprenyl phosphate. PglA, PglJ, PglH (GalNAc-transferases), and PglI (glucosyl-transferase) act sequentially on the PglC product to synthesize the heptasaccharide (3–5). The LLO is then translocated (''flipped'') across the cytoplasmic membrane (CM) into the periplasm by the ABC transporter PglK (6, 7). As a final step, the oligosaccharyltransferase PglB, transfers the oligosaccharide from the lipid to asparagine (N) residues of target proteins in the consensus sequence D/Ex$_1$Nx$_2$S/T, x$_1$, and x$_2$ are any amino acid except proline (8, 9).

1. Schoenhofen IC, et al. (2006) Functional characterization of dehydratase/aminotransferase pairs from *Helicobacter* and *Campylobacter*: Enzymes distinguishing the pseudaminic acid and bacillosamine biosynthetic pathways. *J Biol Chem* 281:723–732.
2. Olivier NB, Chen MM, Behr JR, Imperiali B (2006) In vitro biosynthesis of UDP-N,N′-diacetylbacillosamine by enzymes of the *Campylobacter jejuni* general protein glycosylation system. *Biochemistry* 45:13659–13669.
3. Glover KJ, Weerapana E, Imperiali B (2005) In vitro assembly of the undecaprenylpyrophosphate-linked heptasaccharide for prokaryotic *N*-linked glycosylation. *Proc Natl Acad Sci USA* 102:14255–14259.
4. Linton D, et al. (2005) Functional analysis of the *Campylobacter jejuni N*-linked protein glycosylation pathway. *Mol Microbiol* 55:1695–1703.
5. Weerapana E, Imperiali B (2006) Asparagine-linked protein glycosylation: from eukaryotic to prokaryotic systems. *Glycobiology* 16:91–101.
6. Kelly J, et al. (2006) Biosynthesis of the *N*-linked glycan in *Campylobacter jejuni* and addition onto protein through block transfer. *J Bacteriol* 188:2427–2434.
7. Alaimo C, et al. (2006) Two distinct but interchangeable mechanisms for flipping of lipid-linked oligosaccharides. *EMBO J* 25:967–976.
8. Wacker M, et al. (2002) *N*-linked glycosylation in *Campylobacter jejuni* and its functional transfer into *E. coli*. *Science* 298:1790–1793.
9. Kowarik M, et al. (2006) Definition of the bacterial *N*-glycosylation site consensus sequence. *EMBO J* 25:1957–1966.

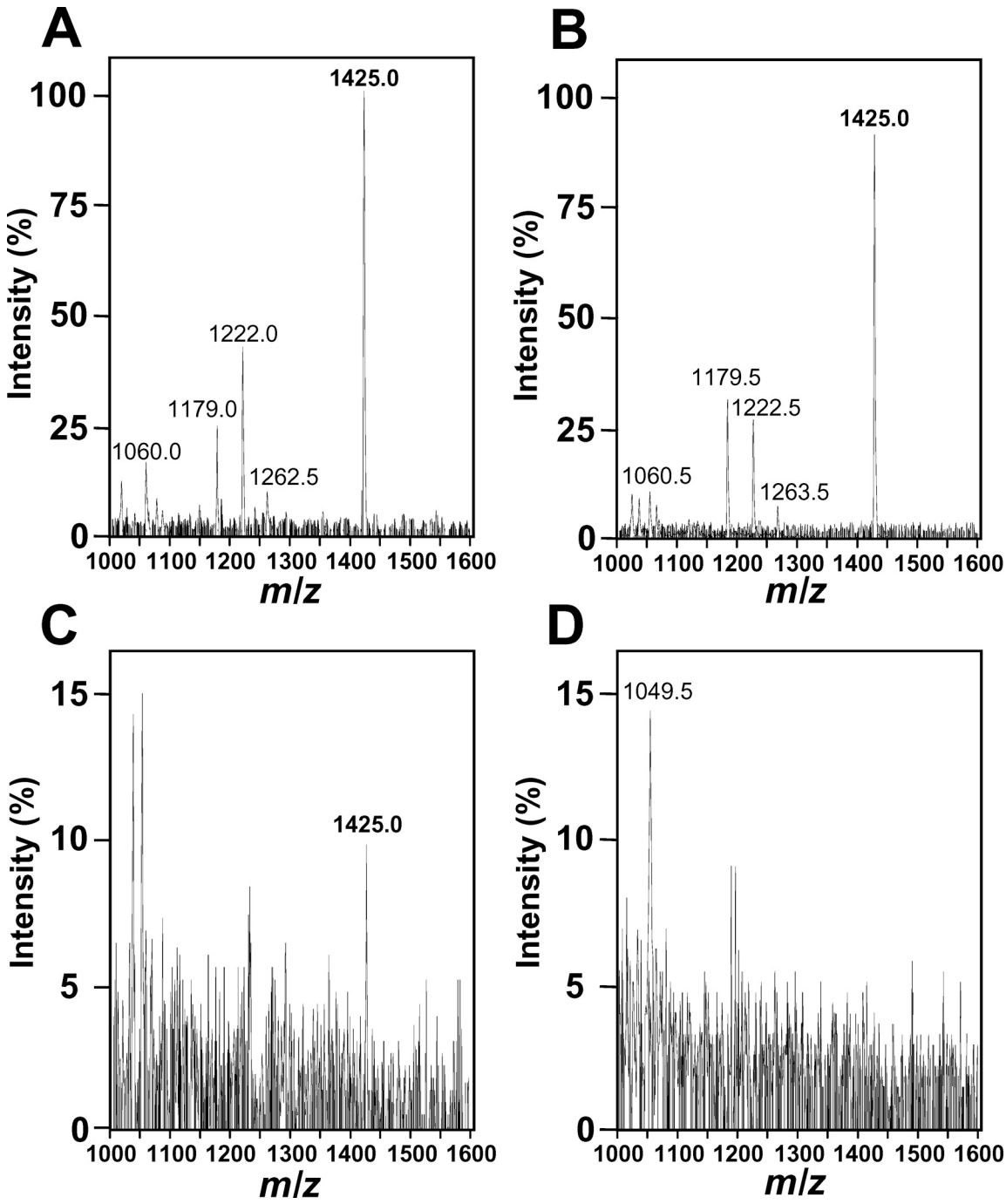

Fig. S2. fOS in different cell fractions of *C. jejuni* 11168. Extracted MS spectra of wild-type fOS were recorded for *C. jejuni* in (*A*) whole cell lysates, (*B*) periplasmic extracts, (*C*) cytoplasmic extracts, and (*D*) membrane preparations. Precursor ions at *m/z* 1425 corresponding to wild-type fOS are in bold. Intensities scales for membrane and cytoplasmic fractions were expressed as an expansion of the wild-type whole cell lysate spectrum scale.

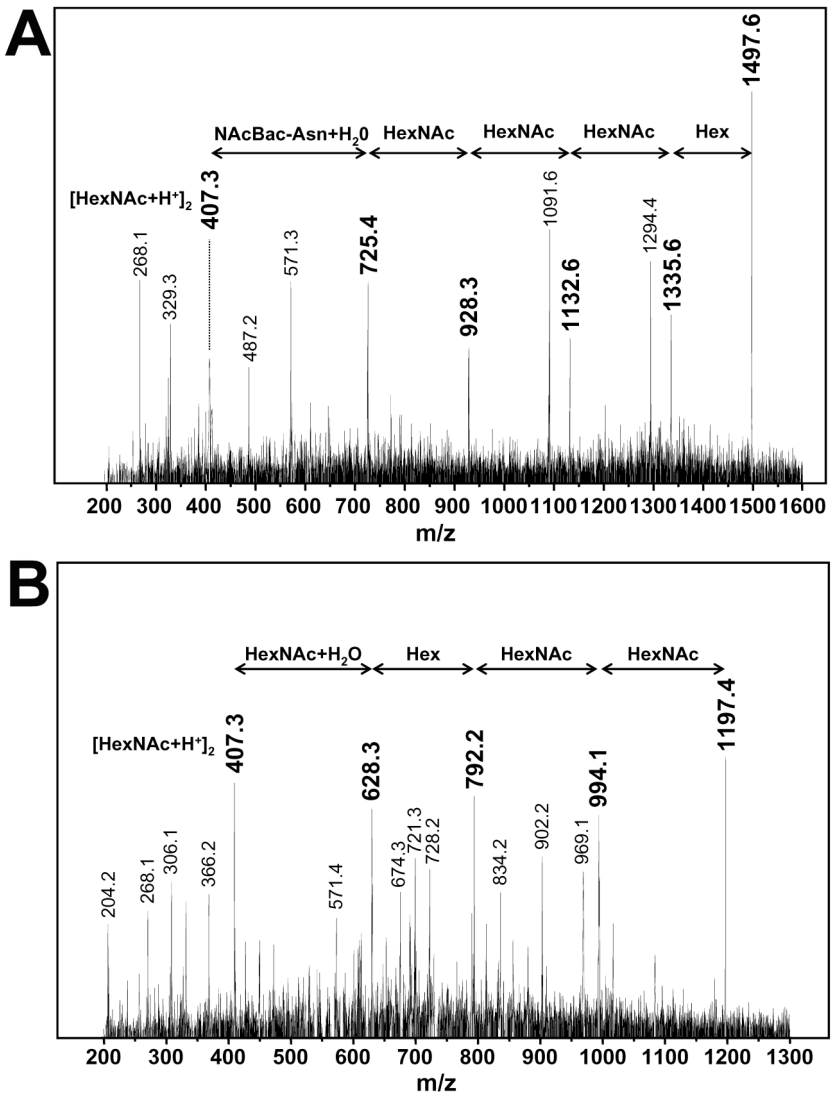

Fig. S3. ESI-MS analysis of free and *N*-linked glycans from the total protein extract of the *C. jejuni pglD* mutant. (*A*) Extracted MS/MS spectrum of the precursor ion at m/z 1497.5. (*B*) Extracted MS/MS spectrum of the precursor ion at m/z 1197.5.

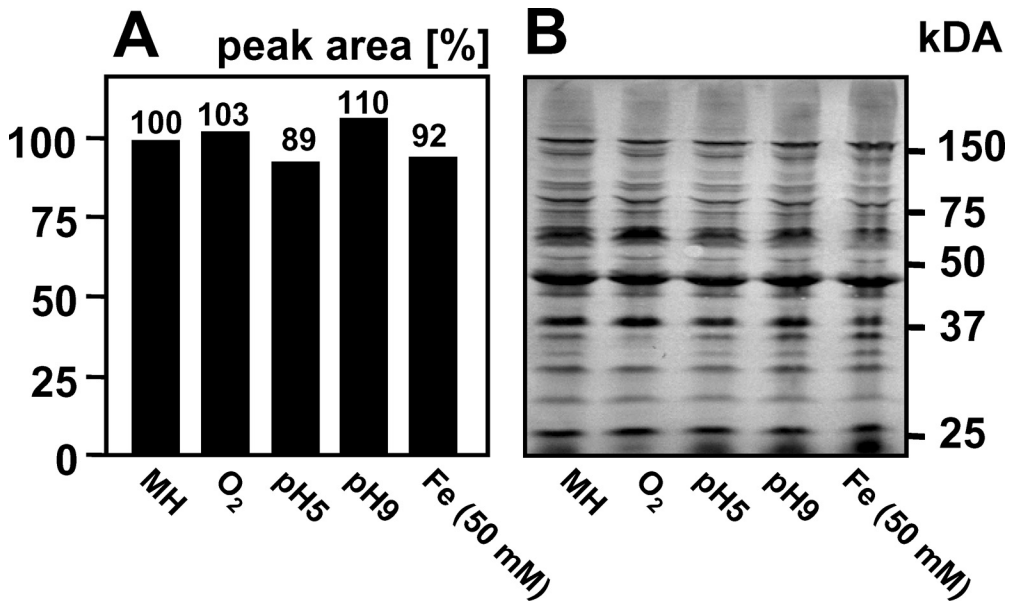

Fig. S4. fOS and *N*-glycan levels in *C. jejuni* 11168 under additional growth conditions. (*A*) The relative amounts of wild-type fOS were determined by sqMS and normalized relative to the level of fOS detected in MH-grown (pH 7.2) wild-type cells. (*B*) The corresponding *N*-linked glycoprotein profiles in whole cell lysates (25 μg/lane) after immunodetection with hR6 antiserum are shown. The masses (in kilodaltons) of marker proteins are indicated on the left.

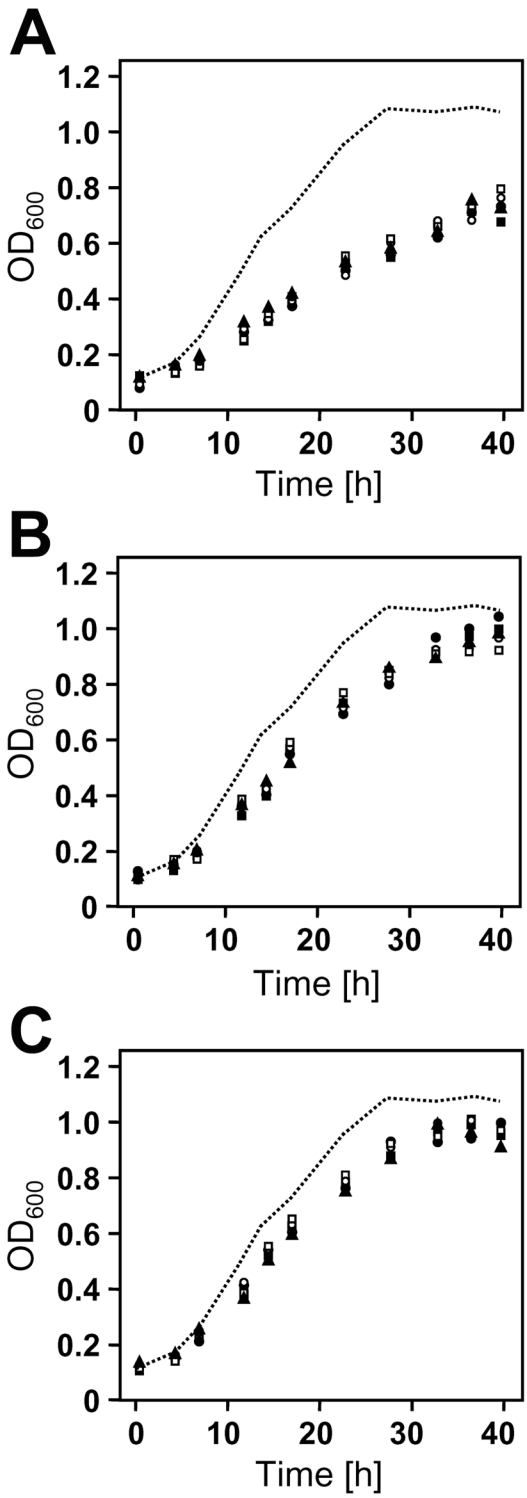

Fig. S5. *C. jejuni* growth phenotypes in the presence of different osmolytes. Growth curves (OD_{600}) were recorded for the wild-type (□); the pglE mutant (●); the *pglF* mutant (○); the *pglB* mutant (■) and the *pglD* mutant (▲) in MH medium supplemented with (*A*) 300 mM sucrose, (*B*) 100 mM KCl and (*C*) 100 mM potassium glutamate. Lines were omitted for clarity reasons. Growth of te mutant strains in MH was comparible to wild-type (dotted lines).

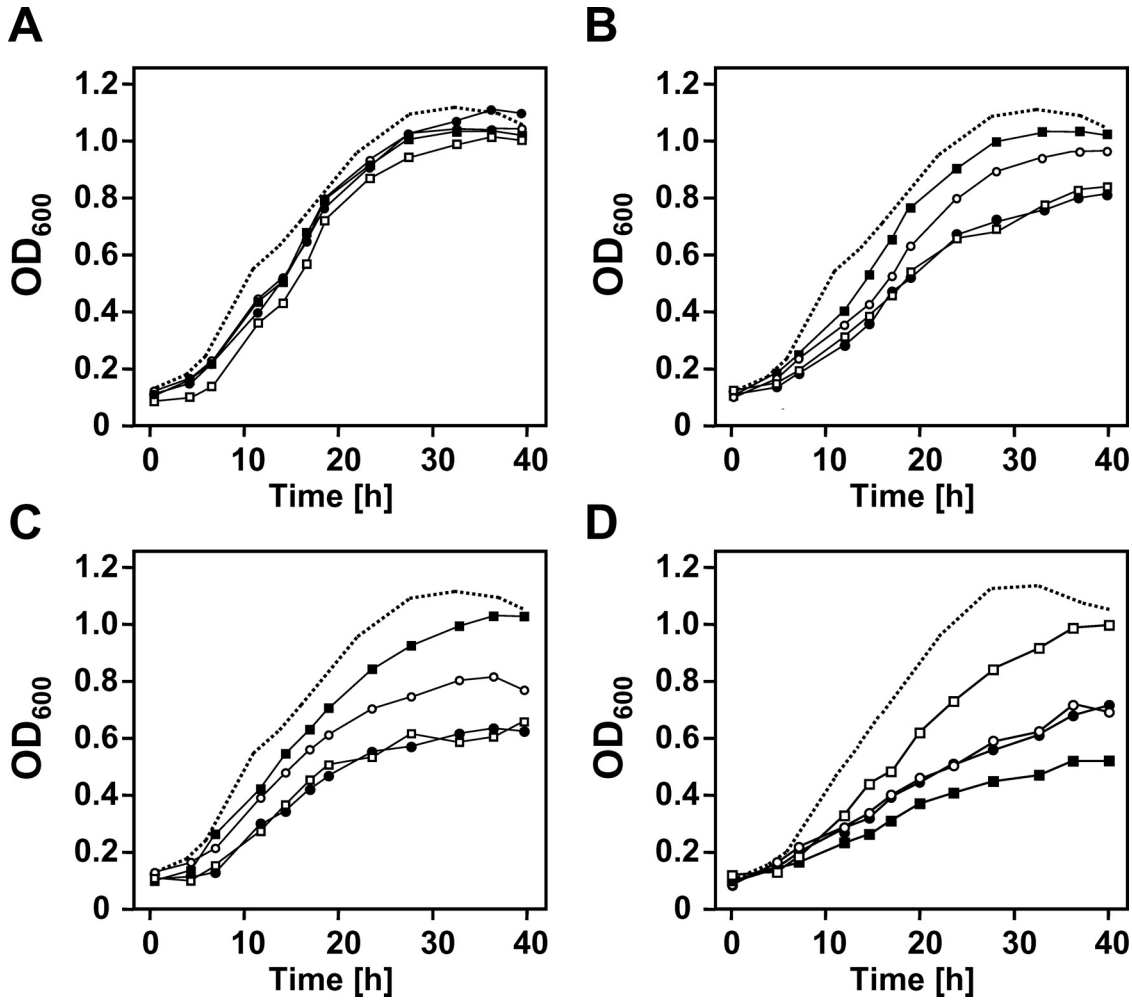

Fig. S6. Growth phenotype of *C. jejuni* 11168 in MH medium supplemented with different NaCl concentrations. Growth curves (OD_{600}) were recorded for the wild-type (■), the *pglB* mutant (●), the complemented *pglB* mutant (*pglB*-pCj-*pglB*) (○), and the *pglB* mutant expressing the mutated *pglB* allele [(^{458}WD^{459} to ^{458}AA^{459}) *pglB*-pCj-$pglB_{mut}$] (□) in MH medium supplemented with (*A*) 10 mM, (*B*) 25 mM, and (*C*) 50 mM NaCl. As a comparison, growth of the wild-type in unsupplemented MH medium is depicted as a dotted line in each growth curve. (*D*) Effects of NaCl on growth of *pglE* and *pglF* mutants: Growth of the *pglE* and the *pglF* mutant in MH was comparable to the wild-type (dotted line). Growth of the strains was also compared in MH supplemented with 100 mM NaCl: Wild-type (□); *pglE* (●); *pglF* (○); and *pglB* (■).

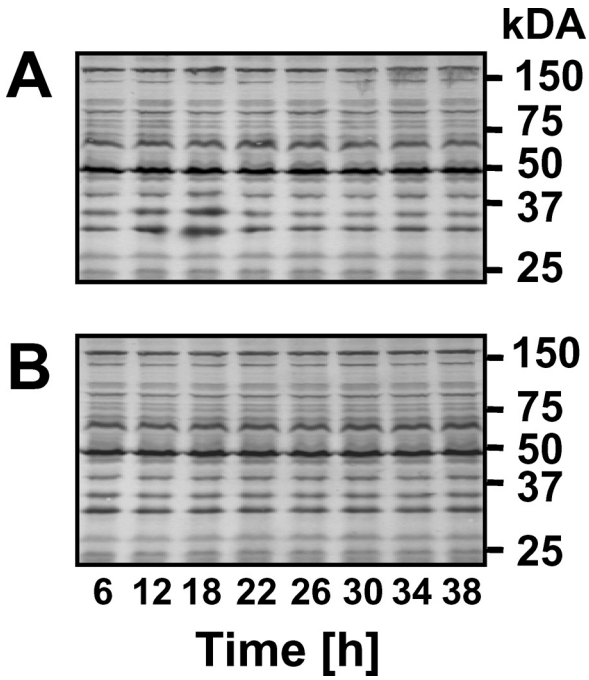

Fig. S7. Growth phase dependent *N*-glycoprotein profiles of *C. jejuni* 11168. *N*-glycoprotein profiles were monitored by immunodetection with hR6 antiserum. Whole cell lysates (25 μg/lane) of cells grown in MH or MH supplemented with 100 mM NaCl were separated on 10% SDS/PAGE. Samples were prepared at the indicated time points. The masses (in kilodaltons) of marker proteins are indicated on the right.

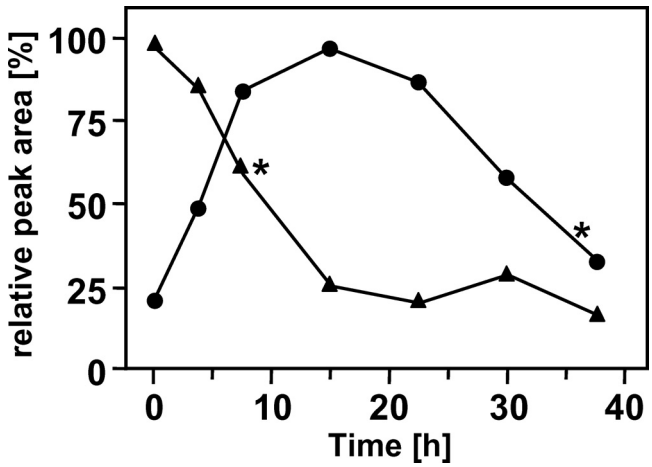

Fig. S8. Effects of changes in NaCl concentrations on fOS production. Relative amounts of fOS were determined over time from whole cell lysates of *C. jejuni* 11168 cells grown in MH after initial growth for 24 h in MH supplemented with 100 mM NaCl (circles); and from whole cell lysates of cells grown on MH supplemented with 100 mM NaCl after initial growth on MH for ≈18 h when maximum amounts of fOS are consistently observed (i.e., OD_{600} of 0.83, triangles). fOS amounts in the culture supernatants were analyzed at the indicated (*) time points.

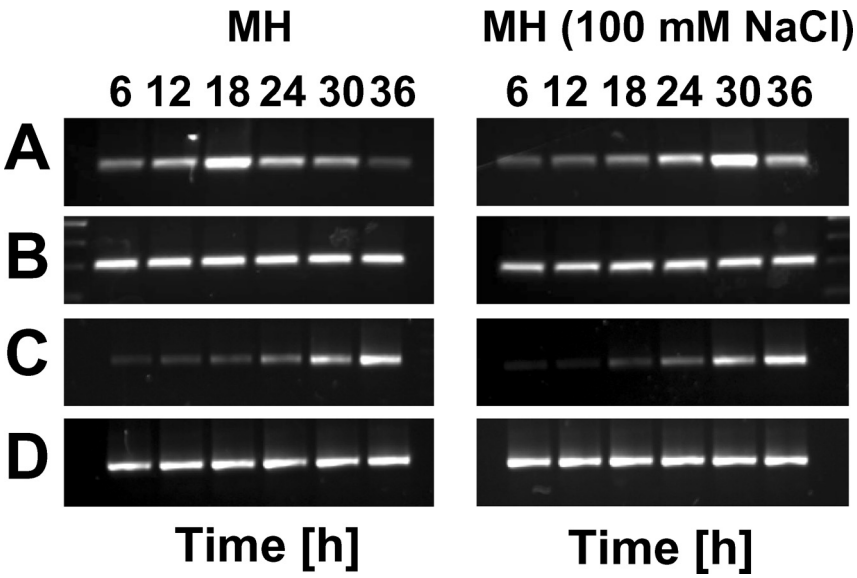

Fig. S9. Time-dependent *pglB* expression. The 1% agarose gels show specific reverse transcriptase-PCR (RT-PCR) products of *pglB* from (*A*) *C. jejuni* 11168 and from (*C*) the *pglB* mutant complemented in *trans* after the 42nd PCR cycle. Total RNA was prepared from cultures grown on MH and MH supplemented with 100 mM NaCl for the indicated times. The 16S rRNA RT-PCR amplification products, taken after the 30th cycle of the PCR served as the invariant standard (*B*, *D*).

Table S1. sqMS-based fOS and *N*-linked glycan quantification in *C. jejuni* 11168

Strain	Function	*N*-linked glycan	%	fOS	%
11168	Wild type (WT)	Heptasaccharide*	100	Heptasaccharide†	100
pglB	Oligosaccharyltransferase	None*	0	nd	0
pglD	Acetyltransferase	Altered heptasaccharide†	50	Hexasaccharide†	20
pglE	Aminotransferase	nd*,‡	0	nd	0
pglF	Dehydratase	nd*,‡	0	nd	0
pglG	Unknown	Heptasaccharide*	108	Heptasaccharide	96
pglH	Processive GalNAc transferase	nd*	0	nd	0
pglI	Glc transferase	Hexasaccharide*	93	Hexasaccharide†	112
pglJ	Second GalNAc transferase	nd*	0	nd	0
pglK	Flippase	nd*	0	Heptasaccharide†	10

nd, not detectable.
*See ref 1.
†See Fig. 1 *A–D*.
‡Low amounts of *N*-linked glycoproteins were immunodetected with hR6 antiserum (see Fig. 1*E*).

1. Kelly J, et al. (2006) Biosynthesis of the *N*-linked glycan in *Campylobacter jejuni* and addition onto protein through block transfer. *J Bacteriol* 188:2427–2434.

Table S2. plasmids and strains used in this study

Strain/plasmid	Relevant genotype and property*	Source or ref.
Plasmid		
pACYC(*pgl*)	Encodes the *C. jejuni pgl* cluster, Cm^R	1
pACYC(pgl_{mut})	Encodes the *C. jejuni pgl* containing mutations W458A and D459A in PglB, Cm^R	1
pWA2	Soluble periplasmic hexa-His-tagged AcrA under control of Tet promoter, in pBR322, Amp^R	2
pWA1	HA-tagged $PglB_{mut}$ cloned in pMLBAD, Tmp^R	2
pMAF10	HA-tagged PglB cloned in pMLBAD, Tmp^R	2
pRY107	*C. jejuni–E. coli* shuttle vector; Kan^R	3
pCE111–28	*C. jejuni* expression vector; plasmid pRY111 with σ^{28} promoter of *flaA*; Cm^R	4
pCj-*pglB*	PglB cloned in pCE111–28, Cm^R; *pglB*, amplified by PCR with oligonucleotides pglB-ZH-1n and HA-XhoI from pWA1; *Xho*I–*Bam*HI- digested PCR products were inserted into the *Campylobacter E. coli* shuttle vector pCE111/28 treated with the same enzymes	This study
pCj-$pglB_{mut}$	$PglB_{mut}$ cloned in pCE111-28, Cm^R; $pglB_{mut}$, amplified by PCR with oligonucleotides pglB-ZH-1n and HA-XhoI from pWA1; *Xho*I-*Bam*HI digested PCR products were inserted into the *Campylobacter-E. coli* shuttle vector pCE111/2 treated with the same enzymes	This study
pRY111(*wlaA-wlaF*)	Encodes part of the *C. jejuni pgl* cluster, Cm^R	5
pRY111(*wlaA-wlaF*) *pglB*::*kan*	pRY111(*wlaA-wlaF*) *pglB*::*kan*, Cm^R, Kan^R; *pglB* knock-out plasmid: 1.2 kb *Eco*RV-derived kanamycin cassette from pRY107 inserted into the unique Site at nt 313 of *pglB* on plasmid pRY111(*wlaA-wlaF*); nonpolar insertion of the kanamycin cassette was verified by sequencing with oligonucleotides FP47 and cj-kan	This study
C. jejuni		
81–176	Clinical isolate	6
11168	Clinical isolate used for genome sequencing	7
11168-*pglA*::Kan	*pglA* mutant; Km^R	8
11168-*pglB*::Kan	*pglB* mutant; Km^R	This study
11168-*pglD*::Kan	*pglD* mutant; Km^R	8
11168-*pglE*::Kan	*pglE* mutant; Km^R	8
11168-*pglF*::Kan	*pglF* mutant; Km^R	9
11168-*pglG*::Kan	*pglG* mutant; Km^R	9
11168-*pglH*::Kan	*pglH* mutant; Km^R	10
11168-*pglI*::Kan	*pglI* mutant; Km^R	9
11168-*pglJ*::Kan	*pglJ* mutant; Km^R	8
11168-*pglK*::Kan	*pglK* mutant; Km^R	9
E. coli		
TOP10	F^- *mcrA* Δ (*mrr-hsdR*MS-*mcrBC*) f80*lac*ZDM15 Δ *lac*X74 *deoR recA araD* Δ (*ara-leu*) *galU galK rpsL endA nupG*	Invitrogen
SCM7	*lacZ trp* Δ (*sbcB-rfb*) *upp rel rpsL* Δ *wec*	11
DH5α	F^-*endA1 hsdR17 supE44 thi-1 recA1* Δ (*argF-lacZYA*)*U169* (80d *lacZ* Δ *M15*) *gyrA96* λ $^-$	Invitrogen
C600 (RK212.2)	*leu thr thi lacY supE44 tonA*; pRK212.2; Amp^R, Tet^R	12

*Amp^R, ampicillin resistance; Cm^R, chloramphenicol resistance; Km^R, kanamycin resistance; Tmp^R, trimethoprim resistance; Tet^R, tetracycline resistance.

1. Wacker M, et al. (2002) *N*-linked glycosylation in *Campylobacter jejuni* and its functional transfer into *E. coli*. *Science* 298:1790–1793.
2. Feldman MF, et al. (2005) Engineering *N*-linked protein glycosylation with diverse O-antigen lipopolysaccharide structures in *Escherichia coli*. *Proc Natl Acad Sci USA* 102:3016–3021.
3. Yao R, Alm RA, Trust TJ, Guerry P (1993) Construction of new *Campylobacter* cloning vectors and a new mutational cat cassette. *Gene* 130:127–130.
4. Larsen JC, Szymanski CM, Guerry P (2004) *N*-linked protein glycosylation is required for full competence in *Campylobacter jejuni* 81-176. *J Bacteriol* 186:6508–6514.
5. Fry BN, et al. (1998) The lipopolysaccharide biosynthesis locus of *Campylobacter jejuni* 81116. *Microbiology* 144:2049–2061.
6. Korlath JA, et al. (1985) A point-source outbreak of campylobacteriosis associated with consumption of raw milk. *J Infect Dis* 152:592–596.
7. Parkhill J, et al. (2000) The genome sequence of the food-borne pathogen *Campylobacter jejuni* reveals hypervariable sequences. *Nature* 403:665–668.
8. Linton D, et al. (2002) Identification of *N*-acetylgalactosamine-containing glycoproteins PEB3 and CgpA in *Campylobacter jejuni*. *Mol Microbiol* 43:497–508.
9. Kelly J, et al. (2006) Biosynthesis of the *N*-linked glycan in *Campylobacter jejuni* and addition onto protein through block transfer. *J Bacteriol* 188:2427–2434.
10. Szymanski CM, Goon S, Allan B, Guerry P (2005) Protein glycosylation in *Campylobacter,* in *Campylobacter: Molecular Cell Biology*, eds Ketley JM, Konkel ME (Horizon Bioscience, Norwich, UK), pp 259–273.
11. Alaimo C, et al. (2006) Two distinct but interchangeable mechanisms for flipping of lipid-linked oligosaccharides. *EMBO J* 25:967–976.
12. Figurski DH, Helinski DR (1979) Replication of an origin-containing derivative of plasmid RK2 dependent on a plasmid function provided in *trans*. *Proc Natl Acad Sci USA* 76:1648–1652.

Table S3. Oligonucleotides used in this study

Oligonucleotide	Sequence 5′-3′	Purpose
FP47	CGCCAGGGTTTTCCCAG	Sequencing
cj-kan	ATCGGGGAAGAACAGTATGTCGAGC	Sequencing
pglB-ZH-1n	ATTAGCGGATCCTACCTGACGCTTTTTATCGC, BamHI site underlined	PCR, cloning
HA-XhoI	TATACTCGAGTTAAGCGTAATCTGGAACATCGTATGG, XhoI site underlined	PCR, cloning
PglBGsp2	AGGAATCACCACCAAAGAAGA	RT-PCR
CS8	AAAACCCTTATTTAGTTTTGTTTGC	RT-PCR
16S-1	AATGGCTTAACCATTAAACTGC	RT-PCR
16S-2	AACTAAATACGTGGGTTGCG	RT-PCR